Front. Phys. 13(6), 132113 (2018)
https://doi.org/10.1007/s11467-018-0843-6

REVIEW ARTICLE

Production cross sections for exotic nuclei with multinucleon transfer reactions

Feng-Shou Zhang[1,2,3,†], **Cheng Li**[1,2], **Long Zhu**[4], **Peiwei Wen**[5]

[1] *The Key Laboratory of Beam Technology of Ministry of Education, College of Nuclear Science and Technology, Beijing Normal University, Beijing 100875, China*
[2] *Beijing Radiation Center, Beijing 100875, China*
[3] *Center of Theoretical Nuclear Physics, National Laboratory of Heavy Ion Accelerator of Lanzhou, Lanzhou 730000, China*
[4] *Sino-French Institute of Nuclear Engineering and Technology, Sun Yat-sen University, Zhuhai 519082, China*
[5] *China Institute of Atomic Energy, Beijing 102413, China*
Corresponding author. E-mail: [†]*fszhang@bnu.edu.cn*
Received July 24, 2018; accepted August 10, 2018

The main progresses in the multinucleon transfer reactions at energies close to the Coulomb barrier are reviewed. After a short presentation of the experimental progress and theoretical progress, the predicted production cross sections for unknown neutron-rich heavy nuclei and the trans-uranium nuclei are presented.

Keywords heavy-ion collisions, multinucleon transfer reactions, exotic nuclei, GRAZING model, DNS model, ImQMD model

PACS numbers 25.70.Hi, 25.70.-z, 24.10.Cn, 25.60.Je

Contents

1 Introduction

To produce new exotic nuclei, there are several methods, such as fission [1, 2], fragmentation/spallation [3–7], and fusion-evaporation reactions [8–10], are widely used in different laboratories over the world. However, these reactions are not possible to produce the new neutron-rich nuclei in the region of trans-uranium and superheavy nuclei [11]. For the region of trans-uranium and superheavy nuclei, the limitations of fusion-evaporation reactions have led to an exploration of multi-nucleon transfer (MNT) reactions between projectile and target at energies around the Coulomb barrier [12–23].

MNT reactions happen in quasi-elastic scattering process, deep inelastic scattering, and partly quasifission reactions. The mechanisms of these reactions are totally different. Deep inelastic scattering was discovered in 1960s. This new mechanism, accompanied with the discovery of quasifission mechanism, greatly promoted the development of heavy ion nuclear reactions. The 70s and 80s of the last century is one of the rapid development period of heavy ion nuclear physics [24, 25]. The interest of multinucleon transfer process existed in quasi-elastic scattering process was renewed in later of 1980s [26, 27]. It was proposed that cold multi-proton transfer can be observed if appropriate dynamical conditions are chosen, which will be helpful for the production of very heavy elements. The mechanisms of deep inelastic transfer and quasi-elastic scattering process are quite different. In deep inelastic transfer reactions, the transfer is mainly result of the friction mechanism, accompanied by large kinematic energy dissipation. The total kinetic energy loss (TKEL) can be hundred MeV, and the angular distribution covers a wide range from positive angle to negative angle, which is called as hot multinu-

*Special Topic: Simplicity, Symmetry, and Beauty of Atomic Nuclei (Eds. Jie Meng, Takaharu Otsuka & Yu-Min Zhao). arXiv: 1809.01775v1.

cleon transfer reaction. The energy dissipation of MNT reaction in quasi-elastic transfer reaction is small, and the angular distribution is concentrated near the grazing angle, which is called as cold multinucleon transfer reaction. For specific reactions, the distinguish of these two kinds of mechanisms is unrealistic. The role of quasifission in multinucleon transfer reaction was indicated in some experimental studies [28, 29]. It is also difficult to distinguish clearly deep inelastic scattering fragments with the quasifission fragments [24, 30].

2 Experimental progress

The discovery of deep inelastic scattering can be traced back to the the pioneering work performed around 1960 at the Yale University Heavy-Ion Linear Accelerator by Kaufmann and Wolfgang [31]. Projectiles including ^{12}C, ^{14}N, ^{16}O, ^{19}F, are used to bombard Al, Cu, Sn, Rh and other targets from near of Coulomb barrier energy to 10 MeV/u. Unexpected phenomena were observed which were not consistent with the previously familiar patterns of compound or direct reactions. Except that angular distribution of the single neutron transfer product ^{15}O is peaked near the grazing angles, the cross section for (pn), (p2n) and (2p3n) transfers are appreciable compared to the single nucleon transfers. The angular distributions of these products are all peaked at forward angles. These experiments indicated that there may be a new reaction mechanism. At that time, they proposed a grazing contact mechanism. It is considered that the bomb nucleus penetrates the target surface without fusion, but rotated along the surface. The contact time is less than half of the rotation period. Nuclear collective excitation and nucleon transfer will happen under the strong friction of this process. Many instructiveness conceptions are proposed in this model, such as the intermediate complex, negative angle rotation, neck formation and elongation, surface tension, friction mechanisms and so on. These conceptions laid the theoretical basis for deep inelastic scattering, which has evolved into the friction model [32, 33], diffusion model and transport model [34], etc.

In the 1960s, due to the limitations of accelerators, people could only use light heavy ion beams (mainly C, N, O). The incident energy for these experiments were conducted at generally 6–10 MeV/u. Many different experimental groups had observed similar multinucleon transfer and forward angle concentration phenomenon [35]. These experimental studies were aimed both at a better understanding of the transfer reaction mechanism and at the production of new isotopes. With the development of accelerators at Dubna, Orsay, and Berkeley in 1970s, heavier ions such as Ar, Kr, Xe, etc., can be accelerated to higher energy. In addition, the development of more advanced experimental techniques were achieved, especially related to correlation measurement such as angle-energy correlation, mass-energy correlation and so on. For example, the development of the magnetic spectrometer in front of the particle telescopes significantly improved the isotopic resolution by Artukh *et al.* [36]. The substantial progress for the experimental studies eventually lead to the establishment of this new reaction mechanism.

One of the most representative examples of deep inelastic scattering is the ^{40}Ar+^{232}Th experiments performed at Dubna [37]. Lately, these experimental results are perfectly interpreted by Wilczyński on the basis of friction theory and scattering into negative angles [38]. The contour plots of double differential cross section as a function of centre of mass angle and total kinetic energy gives quite instructive explanation on this phenomenon, which is often referred to as "Wilczyński plot". The angular distributions of the classical ^{40}Ar+^{232}Th reactions shows an obvious peak around the grazing angle for the fragments close to the projectile. The fragments far from the projectile contributes a smooth part of the angular distribution. The bump and smooth part of the angular distribution corresponds to the high energy (quasi-elastic) and low-energy (deep inelastic) parts, respectively. There are two distinguished ridges in the double differential cross sections contour plot with respect to the energy and angle, which tends to cross near zero degrees. It was reasonably explained by Wilczyński that there are results of the attractive nuclear forces which renders the grazing trajectory towards smaller angles and then to negative angles in deep inelastic process. An important gross feature of deep inelastic transfer reactions is that a broad distribution of product masses can be observed. This is clearly shown by the contour plot of double differential cross section with respect to mass and energy distributions firstly introduced with kinematic coincidence technique [39].

Based on the properties of deep inelastic transfer reaction, it was soon be used to generate new isotopes during the following decades. Between 1969 and 2009, 77 new isotopes had been found by using deep inelastic reactions or multinucleon transfer reactions by different particle identification methods at Dubna, Orsay, Berkeley, and Legnaro [11]. For light particles, it is relatively easy to be identified directly. 47 new neutron-rich light isotopes were discovered by using magnetic spectrometers and direct particle identification method. Between 1969 and 1971, 28 new neutron rich isotopes were detected by Artukh *et al.*, using the U300 heavy-ion cyclotron and magnetic spectrometer combined with a ΔE–E semiconductor telescope including two semiconductor detectors at Dubna [36]. Auger and Guerreau *et al.* identified more

than ten heavier neutron-rich isotopes in deep inelastic reactions induced by ^{40}Ar on ^{238}U with different incident energy, by measuring the time-of-flight of the fragments and using two ΔE measurements with the ALICE facility at Orsay around 1980 [40, 41]. Similar experiment was performed with the Super HILAC accelerator at Berkeley months later, with deep inelastic reactions ^{56}Fe+^{238}U, and thirteen new isotopes were discovered [42]. In Legnaro Tandem XTU-ALPI accelerator, deep transfer reaction ^{82}Se+^{170}Er was performed and ^{170}Dy was deduced from a 163 keV γ-ray spectra [43].

The directly identification of charge and mass of very heavy fragments is very difficult. They cannot be identified by alpha decay tagging because of the spontaneous fission. It is also impossible to directly measure the mass and charge by measurement of energy loss and time-of flight due to the plasma effects and the resulting pulse height deficit at Coulomb barrier region [44]. The missing mass method was firstly introduced to identify the target-like fragments in multi-nucleon transfers. The mass of target-like fragment can be deduced from the two-body kinematic conditions of the projectile-like fragment. Chemical separation approach was also used to identify target-like fragments. Based on these indirect methods, 9 target-like isotopes were determined in multi-nucleon transfer reactions from 1950s to 1990s. As the earliest discovered isotope in multi-nucleon transfer reaction, ^{13}B was determined by measuring protons with a CsI(Tl) scintillating crystal at the Van de Graaff accelerator of the Enrico Fermi Institute for Nuclear Studies [45]. Isotope ^{68}Ni was detected in 1977 with the Q3D spectrometer at the MP tandem of the Max Planck Institute für Kernphysik [46], and ^{69}Ni was detected later with with the double-focusing magnetic spectrometer (BACCHUS) at the MP tandem of Orsay [47]. Zhao *et al.* discovered a new nucleus ^{199}Ir using the transfer reaction ^{198}Pt+^{18}O at 140 MeV with the high-resolution QMG/2 magnetic spectrometer at the Nuclear Structure Facility of Daresbury Laboratory [48]. At the Heavy Ion Research Facility of the Institute of Modern Physics in Lanzhou (HIRFL), five more isotopes of heavy elements, including ^{208}Hg, ^{239}Pa, ^{209}Hg, ^{186}Hf, ^{238}Th, were measured firstly in multinucleon transfer reactions with relatively higher incident energy between 1993 and 1998 by chemical separation method [49–53].

The isotope separation on-line (ISOL) method, original used for identifying fragments for fission and spallation reactions, was also used for distinguishing new isotopes produced in multinucleon transfer reactions. The GSI ISOL facility was operated at the heavy-ion accelerator UNILAC at Darmstadt since 1976 and greatly improved afterwards [54]. During 1980s, 18 new neutron-rich isotopes were identified with different heavy projectiles bombarding on tungsten Ta/W targets or targets with tungsten-tantalum layers [11]. The online mass separator was used to distinguish these new isotopes. The heaviest nucleus among these new isotopes are ^{232}Ac and ^{234}Ac, which are produced with ^{238}U projectile at incident energy 11.4 MeV/u [55]. Around 1990, 3 new isotopes were discovered in deep inelastic reactions by using the ISOL method with the Super HILAC and the OASIS mass separation facility at Berkeley [56, 57].

The cold multi-nucleon transfer and multi-pair transfer were firstly introduced by Oertzen. Based on experimental and theoretical hints, several suggestions were formulated in order to observe the transfer of more than four protons on a ^{248}Cm target based on multiple proton-pair transfer [26, 27]. Transfer of multiple pairs will provide critical information on nucleon-nucleon correlations, especially if measurements are performed below the Coulomb barrier. A series of experiments performed by Corradi *et al.* at the Tandem+ALPI accelerator complex of the Laboratori Nazionali di Legnaro provided lots of evidence about the pair or cluster transfer in multi-nucleon transfer reaction [30]. Reaction ^{40}Ca+^{124}Sn at incident energy 170 MeV around Coulomb barrier was measured with the newly developed time-of-flight magnetic spectrometer at Legnaro in 1996 [58]. The TOF spectrometer was equipped with two microchannel plate detectors and a multiparametric ionization chamber of ΔE–E type, which were used for nuclear charge and energy measurement. A rotating scattering chamber is also connected for measuring the angular distributions at six angles near the grazing one. Angular and Q-value distributions for a large variety of projectile-like charge and mass partitions produced in the reaction were measured clearly. After comparison with independent single-nucleon transfer modes, it was shown that more complex mechanisms shall be considered for the larger drift towards neutron stripping.

With the same experimental setup at Legnaro, multi-nucleon transfer reactions experiments ^{48}Ca+^{124}Sn was performed to clarify the complex mechanisms in 1997 [59]. It was demonstrated that, taking into account only independent single-nucleon transfer modes, experimental isotope cross sections for the $-$2p and +2p channels cannot be described well. The discrepancies can be caused by nucleon pair and cluster degrees of freedom. The MNT detection equipment had been improved a lot during last two decades. The last generation large solid angle magnetic spectrometers PRISMA [60], VAMOS [61] and MAGNEX [62] greatly improved the detection efficiency more than an order of magnitude than previous works. These spectrometers, companied with large gamma arrays allows to detect directly and uniquely gamma-particle and nuclei far from stability, produced via nucleon transfer or deep-inelastic reactions especially in the neutron-rich region [63]. Many multinucleon trans-

fer reactions have given experimental hints on the pair transfer based on above mentioned advanced experimental equipments, such as ^{64}Ni+^{238}U [29], ^{58}Ni+^{208}Pb [64], ^{40}Ca+^{208}Pb [65], ^{64}Ni+^{116}Sn [66], as well as the reaction ^{16}O+^{208}Pb performed at ANU [67].

Due to the available of high-quality $\gamma\gamma$-coincidence data with anti-Compton-shielded multidetector arrays, the resolving of fragments in deep inelastic reactions had become possible in 1990s [68]. Corresponding experimental spectroscopic studies on the emitted fragments improved the study of nuclear structure as a function of isospin and interesting phenomena like shell structure and magic number evolution for neutron-rich nuclei. The gamma spectroscopic studies also inspired the study of N/Z equilibration process in the damped heavy-ion transfer reaction [69]. Based on different kinds of theoretical predictions and experimental hints [69–75], multinucleon transfer reaction was predicted to be able to produce neutron-rich isotopes of heavy nuclei. The studies on this aspect have aroused widely concern. And it seems that MNT reaction is the only current available approach to access the region of heavy neutron-rich nucleus [63]. It is also demonstrated that MNT reaction is a powerful method promising to synthesize neutron rich nuclei around $N = 126$, which are relevant for the rapid neutron capture process and important for the understanding the synthesize of the nuclei heavier than iron in nature [72, 76]. Many MNT experiments have been carried on in recent ten years aimed at production of new isotopes [77–79].

In Ref. [72], it is proposed that for production of possible last "waiting point" heavy neutron-rich nuclei located along the neutron closed shell $N = 126$, multinucleon transfer reactions in low-energy collisions of ^{136}Xe+^{208}Pb shall be explored. This reactions system at different incident energies had been studied at Dubna in 2012 [78] and Argonne National Laboratory in 2015 [80], respectively. Many isotopes had been found in both experiments, especially over 200 projectile-like fragments (PLFs) and target-like fragments (TLFs) were yielded from the these laboratories. These experiments provide great opportunities for the testify of different theoretical models. Another ^{136}Xe+^{208}Pb MNT reaction performed at the Laboratori Nazionali di Legnaro proves the existence of a long-lived isomer in ^{133}Xe [81]. Multinucleon transfer reactions ^{156,160}Gd+^{186}W were also studied recently to investigate $N = 126$ shells [82]. However, no new neutron-rich heavy nuclei was discovered yet.

By virtue of experimental multinucleon transfer reaction ^{136}Xe+^{198}Pt at 7.98 MeV/u, experimental verification was found firstly, which proves the theoretical predictions that MNT would be the suitable tool to populate and characterize neutron-rich isotopes around $N = 126$ shell closure [76]. The experiment was carried out at at GANIL using the large acceptance VAMOS++ spectrometer, and the EXOGAM array with ten CLOVER germanium detectors surrounding the target. In this experiment, the first direct measurements of the absolute production cross sections for a large number of fragments were carried out. There were experimental hints for the production of $N = 126$ nuclides ^{200}W and ^{201}Re in this work. However, these nuclides are deduced from energies and angles of the projectile-like fragments, and the authors did not claim the discovery of these isotopes [11]. The work demonstrated the possibility of producing the new neutron-rich isotopes around $N = 126$ shell closure by MNT reactions at both present and future facilities. After comparison of the production rates in MNT reactions with that from projectile fragmentation reaction ^{208}Pb+Be at 1 GeV/nucleon, it was indicated that the former one is a more optimum way in the production of neutron-rich isotopes around $N = 126$ shell closure. However, by universally comparison of the theoretical expected yields, beam intensities, target thickness and detection efficiencies for Au isotopes produced by multinuclear transfer reaction ^{64}Ni+^{207,208}Pt and fragmentation methods in Ref. [44], it is concluded that fragmentation reactions appear much more favorable for the production of neutron-rich nuclei along the $N = 126$ shell. Finally, it can be concluded that systematic studies to find the optimum projectile-target combinations are critical for the production of nuclei at this region.

For the production of new neutron-rich superheavy nuclei, fragmentation reactions are not applicable, because there are no target or projectile heavy enough. Fusion reactions is also not possible due to that only neutron-deficient heavy nuclei can be produced by this way. Hence, MNT reaction is the only possible way to access these nuclei. It is also predicted in theoretical papers that "asymmetry-exit-channel quasifission reactions" [71] or "inverse quasi-fission" [83] will be potential methods to produce neutron-rich superheavy nuclei. Discussions on the prospects of this method from experimental view can be seen in Refs. [44, 63, 84, 85]. Many experiments have been performed in recent years, such as ^{238}U+^{238}U and ^{238}U+^{248}Cm carried out at the UNILAC accelerator of the GSI [79], ^{136}Xe+^{238}U performed at the INFN Laboratori Nazionali di Legnaro [86]. Important conclusions about the reaction dynamics of these reaction systems have been drawn, but no sizable yield of new neutron-rich heavy isotopes is found yet. One of the key bottlenecks is that it is difficult to identify these high Z elements by current experimental detection methods, due to the Coulomb barrier plasma effects and the resulting pulse height deficit problem [44]. New experimental approaches shall be furthur developed, such as selective laster ionization, Penning trap or multiple reflection time-of-flight mass spectrometer, E-TOP tele-

scopes with calorimeter.

One of the breakthrough in producing new isotopes by multinucleon transfer reaction is the discovery of new neutron-deficient isotopes in 2015. Five new neutron-deficient isotopes, including ^{216}U, ^{219}Np, ^{223}Am, ^{229}Am, and ^{233}Bk were discovered in the MNT reaction ^{48}Ca+^{248}Cm at GSI [87]. The same reaction was performed at GSI in 1986, but no new isotopes were found at that time [88]. The new experiment was performed by using the velocity filter SHIP, and the isotope was identified via the α decay chains. By comparison of the product cross section and experimental efficiency [44], which are experimentally relevant parameter and reflect the event count rate, it is shown that MNT reactions are currently very promising ways for the production of new neutron deficient transuranium isotopes due to their broad excitation functions.

3 Theoretical progress

3.1 Dinuclear system (DNS) model

In the DNS model, after capture happens, nucleon transfer is affected by the relative motion and the transfer process is considered as time-dependent. The evolution of the DNS is a diffusion process along the mass asymmetry degree and simultaneously in the relative distance between the centers of the interacting nuclei. The distribution probability can be obtained by solving a set of master equations numerically in the potential energy surface [89–92].

The total production cross section of a primary fragment with charge Z and mass number A can be calculated as follows:

$$\sigma_{tr}^{DNS}(Z,A,E) = \frac{\pi\hbar^2}{2\mu E}\sum_{l}(2l+1) \times P_c(E,l)P_{tr}^{DNS}(Z,A,E), \quad (1)$$

where P_c is capture probability and $P_{tr}^{DNS}(Z,A,E)$ is the production probability of a fragment, μ is the reduced mass of the colliding system.

Nowadays, the MNT reactions have been proposed to synthesize the exotic nuclei in neutron-rich heavy nuclei, neutron-rich superheavy nuclei, and neutron-deficient heavy nuclei regions. The production cross sections of these exotic nuclei have been extensively predicted by the DNS model. Usually, the neutron-rich heavy exotic nuclei can be produced in the collisions of a neutron-rich stable (^{64}Ni, ^{136}Xe, and ^{176}Yb, etc.) or radioactive (^{132}Sn, ^{139}Xe, and ^{144}Xe, etc) projectile with very heavy target (^{198}Pt, ^{208}Pb, and ^{238}U, etc.). In Fig. 1, the calculated yields of heavy neutron-rich nuclei in the transfer reaction ^{176}Yb+^{238}U are shown [93]. The de-excitation

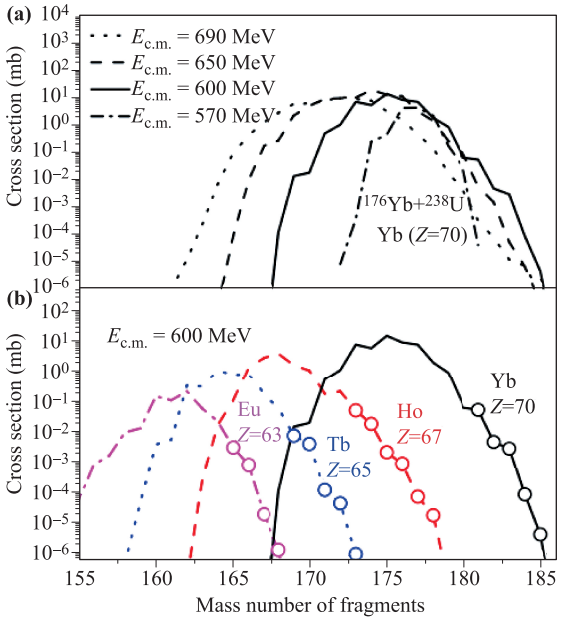

Fig. 1 **(a)** Production cross sections of isotopes of Yb in the transfer reaction ^{176}Yb+^{238}U at $E_{c.m.}$ = 570, 600, 650, and 690 MeV. **(b)** Cross sections for the formation of Eu, Tb, Ho, and Yb isotopes in the reaction ^{176}Yb+^{238}U at $E_{c.m.}$ = 600 MeV. The circles denote the unknown neutron-rich nuclei. Reproduced from Ref. [93].

process of primary fragments are treated with the GEMINI code [94]. Figure 1(a) shows the isotopic distributions at different incident energies. The height of the interaction potential at the touching configuration is about 565 MeV. It is found that cross sections are relatively larger in neutron-rich side when $E_{c.m.}$ = 600 MeV. The calculated cross sections for production of Eu, Tb, Ho, and Yb isotopes in ^{176}Yb+^{238}U reaction at $E_{c.m.}$ = 600 MeV are shown in Fig. 1(b). The calculated production cross sections for the neutron-rich nuclei ^{165,166,167,168}Eu are 2.84 μb, 0.78 μb, 19.64 nb, and 1.36 nb; ^{169,170,171,172,173}Tb are 6.90 μb, 3.70 μb, 0.12 μb, 44.44 nb, and 1.00 nb; ^{173,174,175,176,177,178}Ho are 46.24 μb, 16.83 μb, 2.00 μb, 0.85 μb, 73.75 nb, and 18.08 nb; and ^{181,182,183,184,185}Yb are 53.61 μb, 4.67 μb, 2.85 μb, 84.70 nb, and 4.29 nb, respectively. It can be found that the cross sections of the ^{165}Eu, ^{169}Tb, ^{173}Ho, and ^{181}Yb are quite large for experimental detection.

The neutron-rich radioactive projectile has a larger neutron excess which could significantly improve the production cross section of heavy neutron-rich nuclei. Figure 2 shows the calculated cross sections for reaction products with Z = 72–77 in the collisions of ^{136}Xe, ^{139}Xe, ^{144}Xe, and ^{132}Sn projectiles with ^{208}Pb target [95]. The collision energies were adjusted in such a way that for all cases they are 1.1 times the corresponding potential energies of contact (tip-to-tip) configurations of colliding

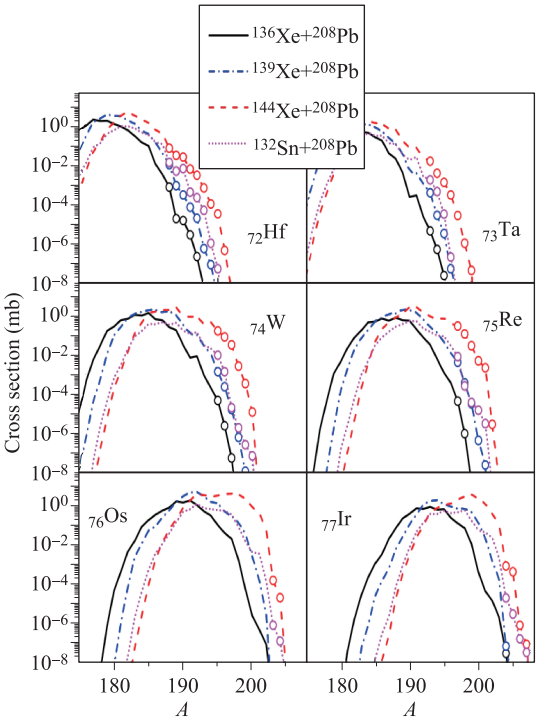

Fig. 2 Production cross sections of isotopes with $Z = 72-77$ in the transfer reactions ^{136}Xe, ^{139}Xe, ^{144}Xe, and ^{132}Sn projectiles with ^{208}Pb. The incident energies are chosen as 1.1 times the Coulomb barrier. The circles denote the unknown neutron-rich nuclei. Reproduced from Ref. [95].

nuclei. It can be seen that radioactive beams enhance the production cross sections of neutron-rich nuclei. As can be seen the curves are shifted to higher mass number region with increasing atomic number of surviving heavy nuclei. In our calculation, it is noticed that many unknown neutron-rich nuclei can be produced with cross section of >0.1 μb in radioactive induced transfer reactions and the production cross sections of unknown neutron-rich nuclei in the reaction ^{144}Xe+^{208}Pb are at least two orders of magnitude larger than those in the reaction ^{136}Xe+^{208}Pb.

The production of exotic nuclei towards the neutron-rich superheavy nuclei has been proposed with damped collisions between two actinide nuclei. In Fig. 3, the production cross sections of Es (+3p), Fm (+4p) and Md (+5p) in ^{238}U+^{248}Cm at $E_{\rm c.m.} = 800$ MeV are calculated by DNS model [93]. One can see a good agreement between theoretical and experimental for larger proton pickup channels in approximately symmetrical system. The cross sections decrease drastically with increasing atomic numbers of the fragments. The survival probabilities of most of the primary fragments are quite low due to a dominant fission channel. The ^{261}Md and ^{262}Md could be synthesized in this reaction with cross sections of about 1.52 nb and 0.17 nb, respectively.

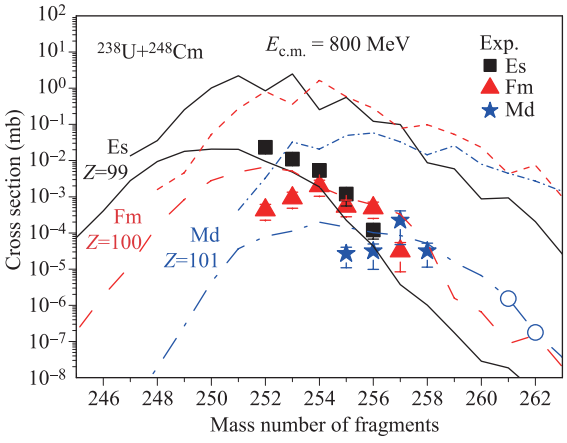

Fig. 3 Cross sections of Es, Fm and Md in ^{238}U+^{248}Cm at $E_{\rm c.m.} = 800$ MeV. The thin and thick lines are distributions of primary and final fragments, respectively. The experimental data are taken from Ref. [96]. The circles denote the unknown nuclei. Reproduced from Ref. [93].

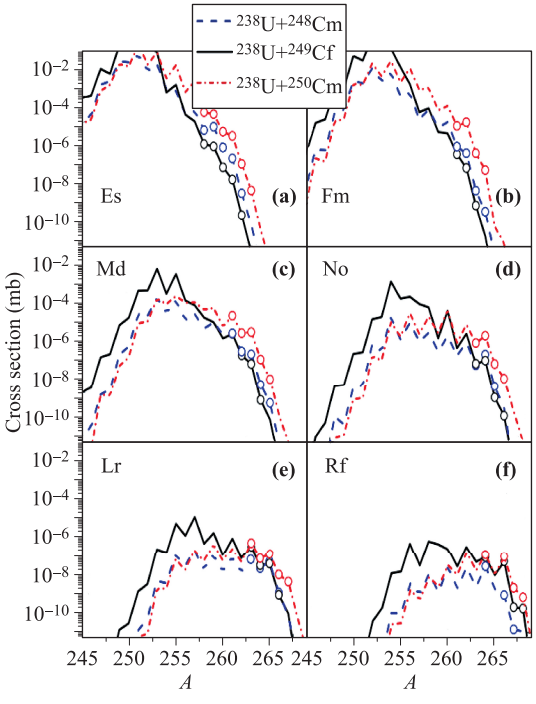

Fig. 4 Cross sections for synthesizing isotopes of the elements with $Z = 99$–104 in transfer reactions ^{238}U+^{248}Cm, ^{238}U+^{249}Cf, and ^{238}U+^{250}Cm. The incident energy $E_{\rm c.m.} = 1.1 \times V_{CN}$. V_{CN} is the interaction potential at the touching point (tip-tip). The circles denote the unknown neutron-rich nuclei. Reproduced from Ref. [97].

In Fig. 4, we show the calculated cross sections for the production of the final reaction products with $Z = 99$–104 in damped collisions of ^{238}U with ^{248}Cm, ^{249}Cf, and ^{250}Cm targets [97]. The collision energies were adjusted in such a way that for all three cases they are

1.1 times the corresponding potential energies of contact (tip-to-tip) configurations of colliding nuclei. The N/Z ratio of the target ^{248}Cm is 1.58, which is higher than 1.54 of ^{249}Cf. The high N/Z ratio target enhances the production cross sections of transtarget neutron-rich nuclei. The reaction ^{238}U+^{248}Cm shows much higher cross sections than ^{238}U+^{249}Cf for the production of unknown neutron-rich isotopes of the element Es. However, for production of the transcalifornium nuclei, two more protons need to be transferred from ^{238}U for the reaction ^{238}U+^{248}Cm in comparison with the reaction ^{238}U+^{249}Cf. Thus, it can be seen that the cross sections of unknown neutron-rich isotopes of the element Rf in the reaction ^{238}U+^{249}Cf become obviously higher than those in the reaction ^{238}U+^{248}Cm.

To produce neutron-deficient actinide nuclei, a neutron-deficient projectile would be better. Figure 5 shows the predicted cross sections for producing unknown neutron-deficient nuclei with Z = 93–97 in the reaction ^{112}Sn+^{238}U [98]. The yields of primary fragments are larger at higher incident energy. However, with increasing excitation energies of primary fragments, more neutrons could be evaporated, which can counteract the increased cross sections of primary fragments. The influence of incident energy in the neutron-deficient region is pronounced. The unknown neutron-deficient nuclei ^{220}Np, ^{221}Np, ^{222}Np, ^{223}Np, and ^{224}Np can be produced in the reaction ^{112}Sn+^{238}U at $E_{\rm c.m.}$ = 550 MeV, with cross sections 0.040, 0.041, 1.0, 0.96, and 2.3 μb, respectively. ^{223}Pu, ^{224}Pu, ^{225}Pu, ^{226}Pu, and ^{227}Pu can be produced with cross sections 0.053, 0.073, 0.30, 0.29, and 1.2 μb, respectively. The predicted cross sections of ^{228}Am, ^{229}Am, ^{231}Cm, ^{232}Cm, ^{232}Bk, and ^{233}Bk are 0.079, 0.088, 0.52, 0.90, 0.022, and 0.066 μb, respectively.

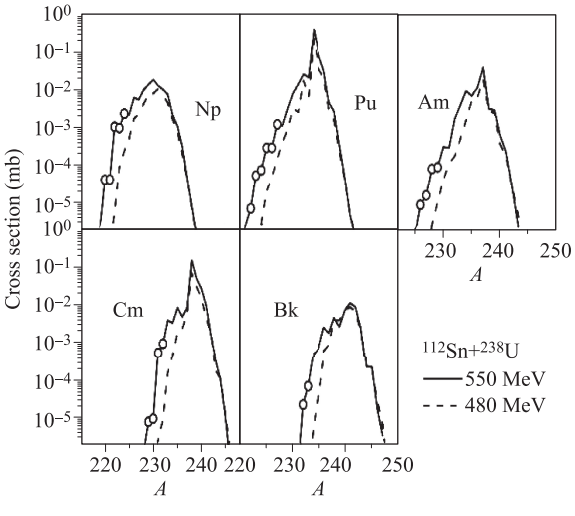

Fig. 5 Calculated cross sections for formation of actinide nuclei with Z = 93–97 in the reaction ^{112}Sn+^{238}U with different incident energies. The circles denote the unknown nuclei. Reproduced from Ref. [98].

3.2 DNS+GRAZING model

GRAZING model is designed in order to evaluate the observable in the MNT reactions that happen in the grazing region [99–102]. In the GRAZING model, exchange of particles is based on well-known form factors of the quantum coupled equations in a mean field approximation, while the colliding nuclei are considered to move on classical trajectories. Similar to the DNS model, the total production cross section can be expressed as

$$\sigma_{tr}^{GRAZING}(Z,A,E) = \frac{\pi\hbar^2}{2\mu E}\sum_l (2l+1) \times(1-P_c(E,l))P_{tr}^{GRAZING}(Z,A,E). \quad (2)$$

It can be seen apparently from Eq. (1) and Eq. (2), the GRAZING model describes transfer reactions without capture, which happen at the scattering process. While DNS model describes the transfer reaction happens in the dinuclear evolution process after capture. These two models represents two kind of transfer mechanisms, which are mutually complementary. Many experimental data indicate that MNT reactions include the direct transfer reaction and DIT reaction. A schematic picture about the subdivision of MNT reactions described by these two models is shown in Fig. 6. In this work, we try to simply combine DNS and GRAZING model (i.e., $\sigma_{tr}^{tot} = \sigma_{tr}^{DNS} + \sigma_{tr}^{GRAZING}$) for description of MNT reactions.

In order to contain simultaneously the scattering and capture process, we combine the DNS and GRAZING model for description of MNT reactions. The isotopic production cross sections of ^{64}Ni+^{238}U at $E_{\rm c.m.}$ = 307.5 MeV are shown in Fig. 7 [103]. For the larger proton

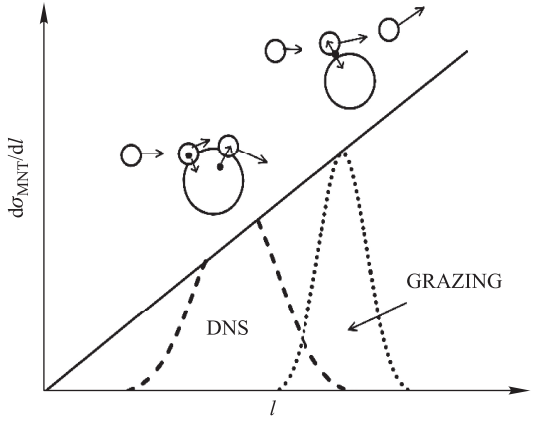

Fig. 6 Schematic picture of the distribution of the cross section differential with respect to the angular momentum l for MNT reactions by the GRAZING model and DNS model. Reproduced from Ref. [103].

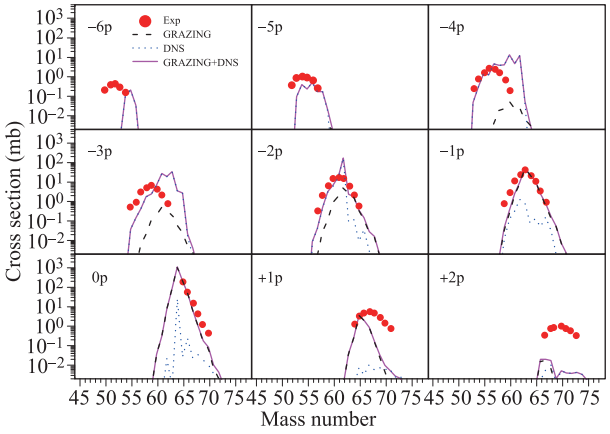

Fig. 7 Isotopic production cross sections (secondary fragments) of ^{64}Ni+^{238}U at $E_{\rm c.m.}$ = 307.5 MeV. The experimental data are from Ref. [29]. Reproduced from Ref. [103].

stripping channels, the DNS model agrees with experimental data better than GRAZING model. While for the −1p to +1p channels, the GRAZING model is better than DNS model. It is hard to describe the transfer reaction with individual scattering or capture mechanism. The GRAZING+DNS model makes a large improvement on −6p to +1p channels. However, the cross sections of +2p channel are substantially underestimated. This combined model should be further developed for describing multinucleon transfer reactions.

3.3 ImQMD model

The ImQMD model is a semiclassical microscopic dynamics model which includes the mean-field and nucleon-nucleon collisions as well as the Pauli principle [104]. In the ImQMD model, each nucleon is represented by a coherent state, and the total N-body wave function is assumed to be the direct product of coherent states. The standard Skyrme force with the omission of spin-orbit term is adopted for describing not only the bulk properties but also the surface properties of nuclei. Simultaneously, the stochastic two-body collision process is added to the time evolution by the Hamilton equation of motion. The final state of the two-body collision process is checked so that it obeys the Pauli principle [105]. The time evolution of $\boldsymbol{r}_i$ and $\boldsymbol{p}_i$ for each nucleon is governed by Hamiltonian equations of motion

$$\dot{\boldsymbol{r}}_i = \frac{\partial H}{\partial \boldsymbol{p}_i}, \quad \dot{\boldsymbol{p}}_i = -\frac{\partial H}{\partial \boldsymbol{r}_i}. \tag{3}$$

The Hamiltonian of the system includes the kinetic energy $T = \sum_i \frac{\boldsymbol{p}_i^2}{2m}$ and effective interaction potential energy

$$H = T + U_{\rm Coul} + U_{\rm loc}, \tag{4}$$

where, $U_{\rm Coul}$ is the Coulomb energy, which is written as a sum of the direct and the exchange contribution

$$U_{\rm Coul} = \frac{1}{2}\iint \rho_p(r)\frac{e^2}{|r-r'|}\rho_p(r')\mathrm{d}r\mathrm{d}r' \tag{5}$$

$$-e^2\frac{3}{4}\left(\frac{3}{\pi}\right)^{1/3}\int \rho_p^{4/3}\mathrm{d}r. \tag{6}$$

ρ_p is the density distribution of protons of the system.

The nuclear interaction potential energy $U_{\rm loc}$ is obtained from the integration of the Skyrme energy density functional $U = \int V_{\rm loc}(\boldsymbol{r})\mathrm{d}\boldsymbol{r}$ without the spin-orbit term, which reads

$$V_{\rm loc} = \frac{\alpha}{2}\frac{\rho^2}{\rho_0} + \frac{\beta}{\gamma+1}\frac{\rho^{\gamma+1}}{\rho 0^{\gamma}} + \frac{g_{sur}}{2\rho_0}(\nabla\rho)^2 + \frac{C_s}{2\rho_0}(\rho^2 - \kappa_s(\nabla\rho)^2)\delta^2 + g_\tau\frac{\rho^{\eta+1}}{\rho_0^{\eta}}. \tag{7}$$

Here $\rho = \rho_n + \rho_p$ is the nucleons density. $\delta = (\rho_n - \rho_p)/(\rho_n + \rho_p)$ is the isospin asymmetry. The density distribution function ρ of a system can be read

$$\rho(r) = \sum_i \frac{1}{(2\pi\sigma_r)^{3/2}}\exp\left[-\frac{(\boldsymbol{r}-\boldsymbol{r}_i)^2}{2{\sigma_r}^2}\right]. \tag{8}$$

The σ_r is the wave-packet width of the nucleon in coordinate space. The ImQMD model is successfully applied to heavy-ion fusion reactions, multinucleon transfer reactions and intermediate-energy fragmentation reactions [105–108]. More descriptions of the ImQMD model please see Refs. [104, 105].

The isotopic production cross sections of ^{136}Xe+^{208}Pb at $E_{\rm c.m.}$ = 450 MeV are shown in Fig. 8. One can see that GRAZING is a suitable model to estimate the production cross sections only for −1p to +2p. It grossly underestimates the production cross section by orders of magnitude in the case of more proton transfers. For the DNS model, the height of peaks kept consistent with experimental data at least on the orders of magnitude for −3p to +2p. For the ImQMD model, the height of peaks always kept consistent with experimental data for −3p to +3p, but the peak widths are usually greater than experimental data especially for $\Delta Z > 0$.

In multinucleon transfer reactions, the nucleons transfer is accompanied by the energy dissipation. The total-kinetic–energy–mass (TKE-mass) distribution can be used to judge the reaction type. Figure 9(a) shows the TKE-mass distributions of ^{136}Xe+^{208}Pb at $E_{\rm c.m.}$ = 450 MeV for primary binary fragments [107]. The total kinetic energy (TKE) is calculated in the center-of-mass system. The central collisions are deep-inelastic reactions. There are a large numbers of nucleons transfers between the projectile and target. The masses distribute in a rather broad range which is from 80 to 250. For

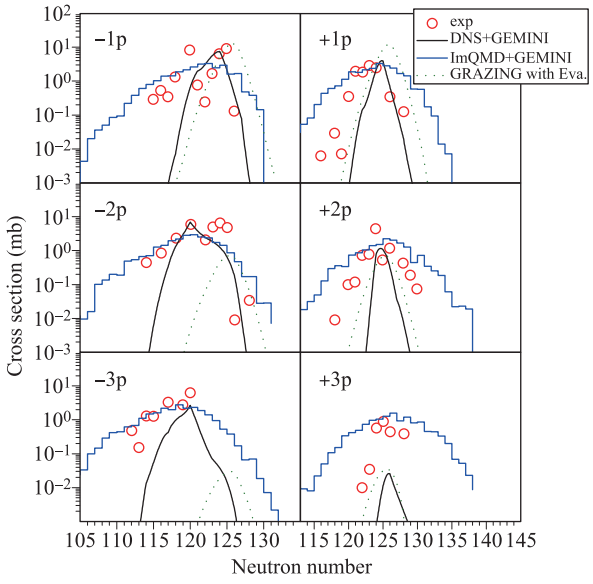

Fig. 8 Isotopic production cross sections (secondary fragments) of ^{136}Xe+^{208}Pb. The experimental data are from Ref. [80]. Reproduced from Ref. [107].

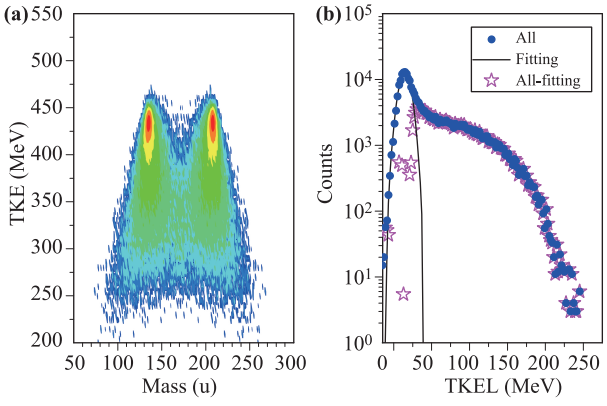

Fig. 9 Calculated TKE-mass distribution and TKEL distribution in ^{136}Xe+^{208}Pb reactions at $E_{\rm c.m.}$ = 450 MeV for primary binary fragments. In right panel, the solid circles denote all the binary events; the solid line denotes the Gaussian fitting for the quasielastic events; the stars are the difference between all the binary events and Gaussian distribution. Reproduced from Ref. [107].

peripheral collisions, there are only a few nucleon transfers with smaller energy loss because the reaction mechanism is dominated by quasielastic collisions. Figure 9(b) shows that the distribution of the total kinetic energy lost (TKEL, i.e., $E_{\rm c.m.}$-TKE) for primary binary events [107]. In Fig. 9(b) one can see that a Gaussian-type distribution appeared at TKEL values lower than 40 MeV, which correspond to quasielastic collision events. Most of the deep-inelastic events are located at TKEL values above 40 MeV. An intense competition between the quasielastic and deep-inelastic reactions caused by

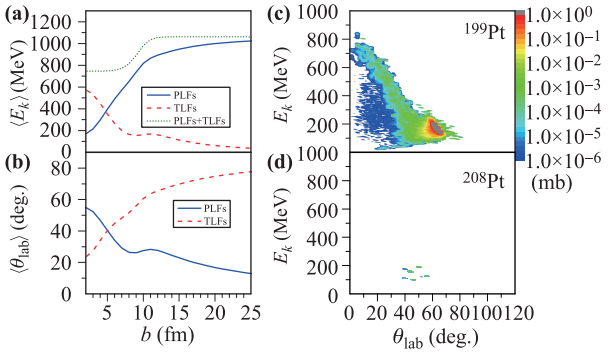

Fig. 10 Left panels: Average kinetic energy $\langle E_k\rangle$ and emission angle $\langle\theta_{\rm lab}\rangle$ of primary fragments for ^{136}Xe+^{198}Pt at $E_{\rm lab}$ = 7.98 MeV/nucleon in the laboratory frame as a function of impact parameters. Right panels: Calculated double differential cross sections (secondary) of ^{199}Pt and ^{208}Pt. Reproduced from Ref. [108].

dynamical fluctuation can be find at the TKEL values near 40 MeV. The TKEL distribution calculated by the ImQMD model is very similar to that measured by experiment from reaction ^{88}Sr+^{176}Yb at an incident energy slightly above the Bass barrier.

In Fig. 10(a), we show the average kinetic energy $\langle E_k\rangle$ of primary fragments for ^{136}Xe+^{198}Pt at $E_{\rm lab}$ = 7.98 MeV/nucleon as a function of the impact parameters [108]. For $12 \leq b$ fm, the reaction mechanism is mainly elastic scattering. No energy is lost in the system after the collisions. In the region of $8 \leq b < 12$ fm, the $\langle E_k\rangle$ value of the target-like fragments (TLFs) is around 150 MeV. While corresponding $\langle E_k\rangle$ value for the Projectile-like fragments (PLFs) decreases rapidly with decreasing impact parameters. The kinetic energy of the projectile dissipate quickly to internal excitation energy in quasielastic and deep-inelastic collisions. For $b < 8$ fm, the $\langle E_k\rangle$ value for TLFs increases rapidly with the decreasing impact parameters. A large amount of energy transfer from the projectile to target occurs in the quasi-fission collisions.

The mean emission angles $\langle\theta_{\rm lab}\rangle$ for the PLFs and TLFs at different impact parameters for ^{136}Xe+^{198}Pt at $E_{\rm lab}$ = 7.98 MeV/nucleon are shown in Fig. 10(b) [108]. The emission angle of light PLFs is significantly affected by nuclear force and Coulomb force. The Coulomb force is dominant when impact parameter is greater than 12 fm. In the region of $8 \leq b < 12$ fm, both the nuclear force and the Coulomb force are important to influence the emission angle of light PLFs. This leads to the result that the values of $\langle\theta_{\rm lab}\rangle$ for PLFs keep around at 28° in quasielastic and in deep-inelastic collisions. For the TLFs, the average emission angle decrease with decreasing impact parameters in the region of $2 < b$ fm.

From Figs. 10(a) and (b), we can distinguish roughly the reaction mechanisms with impact parameters and

emission angles. The corresponding impact parameters for the elastic, quasielastic, deep-elastic and quasifission collisions are in the region of $12 < b$, $10 < b \leq 12$, $8 < b \leq 10$, and $b \leq 8$ fm, respectively. The angles of TLFs in the reaction mechanisms of elastic, quasielastic, deep-inelastic and quasifission distribute in the region of 65°–78°, 60°–65°, 50°–60°, and 23°–50°, respectively. Note that this partition for different reaction mechanisms is rough. The border between different reaction mechanisms gets a bit fuzzy. However, knowing the kinetic energy and the emission angle of a fragment, we can estimate approximately its production mechanism.

Following the above analysis, we can investigate the production mechanism of the new neutron-rich nuclei. The double differential cross sections of ^{199}Pt and ^{208}Pt are shown in Figs. 10(c) and (d) [108]. The ^{199}Pt (+1n) could be produced by three reaction mechanisms. The greatest contribution to producing ^{199}Pt is quasielastic collisions (grey area). The corresponding emission angles are from 60° to 70° and kinetic energy is around 150 MeV. The fragments with emission angles from 40° to 60° and kinetic energy around 150 MeV is produced primarily in the deep-inelastic collisions. The fragments with smaller emission angles and kinetic energy larger than 200 MeV is mainly produced in quasifission mechanism. The very neutron-rich isotope ^{208}Pt (+10n) is produced in deep-inelastic reactions. The exotic neutron-rich nuclei cannot be generated in quasielastic and quasifission collisions. Because in the quasielastic collisions, only a few nucleons could be transferred. While for the quasifission collisions, large excitation energy is obtained in energy dissipation processes which causes that the primary fragments evaporate more neutrons in the deexcitation processes.

Figure 11 shows that the final production cross section distributions for TLFs [108]. From Fig. 11, one can see that about 50 new neutron-rich nuclei have survived after the deexcitation processes. The production cross sections of these new neutron-rich nuclei are mainly located in the region of 10^{-3}–10^{-6} mb. Actually, in the Ref. [76], these new neutron-rich nuclei were not detected because the detection limit of the experiment is 10^{-2} mb.

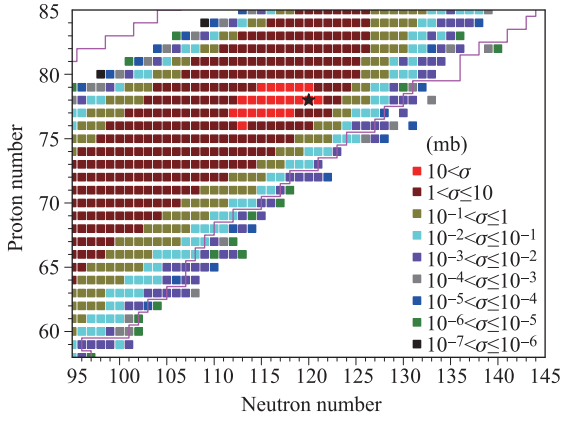

Fig. 11 Calculated production cross section distributions for the secondary fragments in the ^{136}Xe+^{198}Pt reaction. The folding lines denote the boundary of known nuclei. The star denotes the position of the target. Reproduced from Ref. [108].

4 Predicated cross sections for new exotic nuclei

The predicted production cross sections of the new nuclei in MNT reactions with stable projectile-target combination are listed in Table 1. The transfer reactions ^{136}Xe+^{186}W [109], ^{136}Xe+^{208}Pb [95], ^{136}Xe+^{248}Cm [98], and ^{112}Sn+^{238}U [98] are calculated within the framework of the DNS model. The new isotopes in ^{136}Xe+^{198}Pt [108] reaction are predicted by using the ImQMD model. The ^{136}Xe+^{186}W reaction can produce the new neutron-rich nuclei with $Z = 70$–72. The transfer reaction of ^{136}Xe+^{208}Pb at $E_{\mathrm{c.m.}} = 465$ MeV can produce the new neutron-rich nuclei with atomic number form 72 to 75. The ^{136}Xe+^{248}Cm reaction at $E_{\mathrm{c.m.}} = 510$ MeV can produce the new neutron-rich trans-uranium nuclei with $Z = 92 - 96$. The neutron-deficient ^{112}Sn with ^{238}U at $E_{\mathrm{c.m.}} = 550$ MeV can produce the new neutron-deficient trans-uranium nuclei with atomic number from 93 to 97. The reaction of ^{136}Xe+^{198}Pt at $E_{\mathrm{c.m.}} = 643$ MeV can produce the new neutron-rich nuclei with Z from 59 to 82.

Table 1 Predicted cross sections of new isotopes in MNT reactions from the DNS and ImQMD model.

Reactions	Isotopes	Cross section (mb)
^{136}Xe+^{186}W, $E_{\mathrm{c.m.}} = 406$ MeV		DNS Cal.
	^{181}Yb	6.659×10^{-2}
	^{182}Yb	2.135×10^{-2}
	^{183}Yb	2.030×10^{-3}
	^{184}Yb	1.813×10^{-5}
	^{185}Yb	7.659×10^{-7}
	^{186}Yb	4.265×10^{-7}
	^{185}Lu	2.160×10^{-4}
	^{186}Lu	4.037×10^{-5}
	^{187}Lu	1.289×10^{-5}
	^{188}Lu	2.270×10^{-7}
	^{188}Hf	1.481×10^{-4}
	^{189}Hf	1.028×10^{-5}
	^{190}Hf	3.061×10^{-6}
^{136}Xe+^{208}Pb, $E_{\mathrm{c.m.}} = 465$ MeV		DNS Cal.
	^{188}Hf	6.958×10^{-4}
	^{189}Hf	1.710×10^{-5}
	^{190}Hf	1.368×10^{-5}
	^{191}Hf	2.543×10^{-6}

Table 1 (continued)

Reactions	Isotopes	Cross section (mb)
	^{192}Hf	2.032×10^{-7}
	^{193}Ta	4.048×10^{-6}
	^{194}Ta	4.668×10^{-7}
	^{195}Ta	2.200×10^{-8}
	^{195}W	4.739×10^{-5}
	^{196}W	2.472×10^{-6}
	^{197}W	5.820×10^{-8}
	^{197}Re	4.413×10^{-5}
	^{198}Re	1.003×10^{-6}
^{136}Xe+^{248}Cm, $E_{\mathrm{c.m.}} = 510$ MeV		DNS Cal.
	^{244}U	3.543×10^{-4}
	^{245}U	4.610×10^{-5}
	^{246}U	1.423×10^{-7}
	^{247}U	2.659×10^{-8}
	^{248}U	2.032×10^{-8}
	^{245}Np	1.044×10^{-3}
	^{246}Np	1.706×10^{-4}
	^{247}Np	1.897×10^{-6}
	^{248}Np	8.901×10^{-7}
	^{249}Np	2.438×10^{-7}
	^{248}Pu	1.524×10^{-4}
	^{249}Pu	4.610×10^{-5}
	^{250}Pu	6.282×10^{-6}
	^{251}Pu	2.457×10^{-6}
	^{249}Am	3.362×10^{-4}
	^{250}Am	1.934×10^{-4}
	^{251}Am	1.387×10^{-4}
	^{252}Am	2.377×10^{-5}
	^{253}Cm	1.251×10^{-4}
	^{254}Cm	5.188×10^{-5}
	^{255}Cm	9.067×10^{-6}
^{112}Sn+^{238}U, $E_{\mathrm{c.m.}} = 550$ MeV		DNS Cal.
	^{220}Np	4.046×10^{-5}
	^{221}Np	4.115×10^{-5}
	^{222}Np	1.032×10^{-3}
	^{223}Np	9.612×10^{-4}
	^{224}Np	2.321×10^{-3}
	^{222}Pu	6.793×10^{-6}
	^{223}Pu	5.258×10^{-5}
	^{224}Pu	7.271×10^{-5}
	^{225}Pu	2.902×10^{-4}
	^{226}Pu	2.899×10^{-4}
	^{227}Pu	1.222×10^{-3}
	^{226}Am	8.397×10^{-6}
	^{227}Am	1.503×10^{-5}
	^{228}Am	7.896×10^{-5}
	^{229}Am	8.820×10^{-5}
	^{229}Cm	7.720×10^{-6}
	^{230}Cm	9.225×10^{-6}
	^{231}Cm	5.181×10^{-4}
	^{232}Cm	9.033×10^{-4}

Table 1 (continued)

Reactions	Isotopes	Cross section (mb)
	^{232}Bk	2.169×10^{-5}
	^{233}Bk	6.574×10^{-5}
^{136}Xe+^{198}Pt, $E_{\mathrm{c.m.}} = 643$ MeV		ImQMD Cal.
	^{156}Pr	7.000×10^{-3}
	^{157}Pr	1.475×10^{-3}
	^{158}Pr	1.435×10^{-3}
	^{159}Pr	1.427×10^{-2}
	^{160}Pr	5.893×10^{-3}
	^{162}Nd	1.440×10^{-6}
	^{166}Sm	1.701×10^{-6}
	^{169}Eu	3.668×10^{-3}
	^{170}Eu	1.333×10^{-3}
	^{171}Eu	7.671×10^{-4}
	^{172}Gd	1.964×10^{-3}
	^{173}Tb	7.281×10^{-3}
	^{174}Tb	1.950×10^{-3}
	^{175}Tb	1.375×10^{-5}
	^{175}Dy	2.417×10^{-3}
	^{176}Dy	5.629×10^{-6}
	^{177}Dy	1.701×10^{-3}
	^{178}Dy	1.960×10^{-3}
	^{179}Dy	3.928×10^{-6}
	^{177}Ho	7.389×10^{-3}
	^{178}Ho	3.530×10^{-4}
	^{179}Ho	5.104×10^{-6}
	^{179}Er	1.108×10^{-2}
	^{180}Er	9.413×10^{-5}
	^{181}Er	2.218×10^{-3}
	^{182}Er	1.060×10^{-5}
	^{182}Tm	4.233×10^{-3}
	^{183}Tm	6.283×10^{-6}
	^{184}Tm	2.488×10^{-3}
	^{186}Yb	2.035×10^{-3}
	^{189}Lu	3.665×10^{-6}
	^{191}Hf	5.717×10^{-3}
	^{192}Hf	8.504×10^{-3}
	^{193}Hf	3.355×10^{-3}
	^{194}Hf	4.254×10^{-5}
	^{200}Re	1.019×10^{-2}
	^{201}Re	4.785×10^{-4}
	^{202}Re	1.479×10^{-3}
	^{203}Re	2.356×10^{-5}
	^{204}Os	2.691×10^{-3}
	^{205}Os	9.385×10^{-4}
	^{207}Os	3.534×10^{-5}
	^{207}Ir	2.488×10^{-3}
	^{209}Pt	3.545×10^{-3}
	^{211}Pt	3.522×10^{-4}
	^{211}Au	1.375×10^{-5}
	^{221}Pb	3.915×10^{-4}
	^{222}Pb	1.178×10^{-6}

In addition, radioactive ion beam facilities can provide very neutron-rich projectiles. Some facilities, such as the high-intensity heavy-ion accelerator facility (HIAF) in China, have a plan to produce new heavy neutron-rich nuclei with intense secondary beams of exotic radioactive nuclei by the MNT reactions. The production mechanism of heavy neutron-rich nuclei is also investigated by using the NNT reactions with radioactive projectiles. We find that neutron-rich radioactive beams can improve significantly the production cross sections of neutron-rich nuclei, see Refs. [95, 98, 109, 110].

5 Conclusions and perspectives

The multinucleon transfer process will be one promising approach for producing neutron-rich light nuclei, neutron-rich heavy nuclei, neutron-rich superheavy nuclei, and neutron-deficient heavy nuclei.

For producing unknown nuclei in multinucleon transfer reactions, the main difficulties in the experiments would be how to separate a given nucleus from other transfer products. Coupling large gamma arrays to the new generation large solid angle spectrometers can give a full identification of reaction products. In the future, with the increasing efficiency of experimental process, the products with very low production cross sections can be detected.

The multinucleon transfer reactions with stable combinations can be the candidates for producing unknown neutron-rich nuclei. However, the production cross section decreases strongly with the increasing neutron number of objective nuclei. Therefore, the production of neutron-rich nuclei far from the stability line with stable beam induced transfer reaction is very hard. Radioactive beam induced reactions could enhance the cross sections strongly. In present experimental facilities, the beam intensities of radioactive beams are still very low. With the development of modern radioactive equipment, the radioactive beams could be favorable for producing neutron-rich nuclei far from the stable line.

The multinucleon transfer process is promising for producing neutron-rich SHN, which can reach the island of stability. Theoretical predictions show that within the collisions of actinide nuclei, the trans-actinide nuclei can be produced. And the yields decrease strongly with the increasing charge number of objective SHN. It seems like that it is almost impossible to produce SHN with $Z = 114$ or larger. Recently, experimental observation of alpha decay energies reaching as high as 12 MeV suggests the production of high atomic number, which implies that the production cross sections of SHN through multinucleon transfer reactions were underestimated by theoretical models. Experimentally, the improvement of catcher array with high granularity, better energy resolution, and linear energy response can search the SHN with very low production rate. Theoretically, according to the experimental results, one should make more accurate predictions of fission barrier in SHN region, which strongly influence the survival probability of products. Furthermore, the shell effects, dynamical process of fission, and beta decay feeding by the neighboring nuclei should also be investigated for better predictions of production rates.

Until now, the observed products in multinucleon transfer reactions are around the projectile and the target. For producing neutron-rich superheavy nuclei, such as approaching the island of stability, plenty of nucleons should be transferred. Due to lack of experimental data, the prediction ability of models is limited for production of neutron-rich superheavy nuclei, although most of present theoretical models can show good descriptions of available experimental data. Therefore, more experiments are necessary of producing trans-actinide nuclei in multinucleon transfer reactions, which could provide information for constraining the models. For development of the macroscopic models, appropriate collective degrees of freedom should be considered. For example, during the deep inelastic collisions, the collective vibration probably plays an important role on charge equilibration process. Also, because of oscillations in collision process, bremsstrahlung approach would emit photons, which could lower the effective incident energy. The double nucleon transfer is very important in transfer channels. For most of theoretical models, the description of paring mode is lack, which limits the abilities of prediction. Therefore, the improvement of theoretical framework from the structure point is necessary.

Acknowledgements We warmly thank Prof. A. Arima for the encouragement on transport model on heavy ion collisions. F. S. Zhang thanks Y. Abe, S. Ayik, D. Boilley, L. W. Chen, D. Q. Fang, Z. G. Gan, S. Heinz, Y. G. Ma, J. Meng, B. A. Li, C. J. Lin, W. P. Liu, Z. Liu, W. Loveland, Z. Z. Ren, W. Q. Shen, X. D. Tang, B. Tsang, Yu. S. Tsyganov, M. Veselsky, J. S. Wang, C. Y. Wong, G. Q. Xiao, Z. G. Xiao, F. R. Xu, Y. L. Ye, W. L. Zhan, H. Q. Zhang, Y. H. Zhang, E. G. Zhao, Y. M. Zhao, S. G. Zhou, X. H. Zhou, and S. Zhu for valuable discussions on multinucleon transfer reactions. This work was supported by the National Natural Science Foundation of China under Grants Nos. 11635003, 11025524, 11161130520, 11605270, 11605296, 11805015, and 11805280; the National Basic Research Program of China under Grant No. 2010CB832903; the European Commission's 7th Framework Programme (Fp7-PEOPLE-2010-IRSES) under Grant Agreement Project No. 269131; the China Postdoctoral Science Foundation (Grant Nos. 2016M600956, 2017M621035, and 2018T110069); the Beijing Postdoctoral Re-

search Foundation (2017-zz-076); and the Natural Science Foundation of Guangdong Province, China (Grant No. 2016A030310208).

References and notes

1. H. Mach, A. Piotrowski, R. L. Gill, R. F. Casten, and D. D. Warner, Identification of Four New Neutron-Rich Rare-Earth Isotopes, *Phys. Rev. Lett.* 56, 1547 (1986)
2. G. Engler, Y. Nir-El, M. Shmid, and S. Amiel, Half-life measurements of Rb, Sr, Y, Cs, Ba, La and Ce isotopes with $A = 91 - 98$ and $A = 142 - 149$, *Phys. Rev. C* 19, 1948 (1979)
3. J. Kurcewicz, F. Farinon, H. Geissel, S. Pietri, C. Nociforo, et al., Discovery and cross-section measurement of neutron-rich isotopes in the element range from neodymium to platinum with the FRS, *Phys. Lett. B* 717, 371 (2012)
4. O. B. Tarasov, D. J. Morrissey, A. M. Amthor, T. Baumann, D. Bazin, et al., Evidence for a Change in the Nuclear Mass Surface with the Discovery of the Most Neutron-Rich Nuclei with $17 \leq Z \leq 25$, *Phys. Rev. Lett.* 102, 142501 (2009)
5. F. S. Zhang and L. X. Ge, Nuclear Fragmentation, Science Press, Beijing, 1998
6. F. S. Zhang and E. Suraud, Analysis of multifragmentation in a Boltzmann–Langevin approach, *Phys. Rev. C* 51, 3201 (1995)
7. F. S. Zhang and E. Suraud, Boltzmann–Langevin equation, dynamical instability and multifragmentation, *Phys. lett. B* 319, 35 (1993)
8. Y. Aritomo, T. Wada, M. Ohta, and Y. Abe, Fluctuation-dissipation model for synthesis of superheavy elements, *Phys. Rev. C* 59, 796 (1999)
9. C. Y. Wong, Interaction barrier in charged-particle nuclear reactions, *Phys. Rev. Lett.* 31, 766 (1973)
10. H. Lü, D. Boilley, Yasuhisa Abe, and C. W. Shen, Synthesis of superheavy elements: Uncertainty analysis to improve the predictive power of reaction models, *Phys. Rev. C* 94, 034616 (2016)
11. M. Thoennessen, The Discovery of Isotopes: A Complete Compilation, Springer International Publishing, US, 2016
12. S. Ayik, O. Yilmaz, B. Yilmaz, A. S. Umar, A. Gokalp, G. Turan, and D. Lacroix, Quantal description of nucleon exchange in a stochastic mean-field approach, *Phys. Rev. C* 91, 054601 (2015)
13. S. Ayik, K. Washiyama, and D. Lacroix, Fluctuation and dissipation dynamics in fusion reactions from a stochastic mean-field approach, *Phys. Rev. C* 79, 054606 (2009)
14. R. Yanez and W. Loveland, Predicting the production of neutron-rich heavy nuclei in multinucleon transfer reactions using a semi-classical model including evaporation and fission competition, GRAZING-F, *Phys. Rev. C* 91, 044608 (2015)
15. E. Vigezzi and A. Winther, On the application of complex trajectories to direct heavy-ion reactions, *Ann. Phys. (NY)* 192, 432 (1989)
16. L. Corradi, A. M. Stefanini, D. Ackermann, S. Beghini, G. Montagnoli, C. Petrache, F. Scarlassara, C. H. Dasso, G. Pollarolo, and A. Winther, Multinucleon transfer reactions in ^{32}S+^{208}Pb close to the Coulomb barrier, *Phys. Rev. C* 49, 2875(R) (1994)
17. L. Corradi, A. M. Vinodkumar, A. M. Stefanini, E. Fioretto, G. Prete, S. Beghini, G. Montagnoli, F. Scarlassara, G. Pollarolo, F. Cerutti, and A. Winther, Light and heavy transfer products in ^{58}Ni+^{208}Pb at the Coulomb barrier, *Phys. Rev. C* 66, 024606 (2002)
18. O. Beliuskina, S. Heinz, V. Zagrebaev, V. Comas, C. Heinz, et al., On the synthesis of neutron-rich isotopes along the $N = 126$ shell in multinucleon transfer reactions, *Eur. Phys. J. A* 50, 161 (2014)
19. T. Welsh, W. Loveland, R. Yanez, J. S. Barrett, E. A. McCutchan, et al., Modeling multi-nucleon transfer in symmetric collisions of massive nuclei, *Phys. Lett. B* 771, 119 (2017)
20. V. Zagrebaev and W. Greiner, Shell effects in damped collisions: A new way to superheavies, *J. Phys. G Nucl. Part. Phys.* 34, 2265 (2007)
21. S. Wuenschel, K. Hagel, M. Barbui, J. Gauthier, X. G. Cao, et al., Experimental survey of the production of α-decaying heavy elements in ^{238}U +^{232} Th reactions at 7.5–6.1 MeV/nucleon, *Phys. Rev. C* 97, 064602 (2018)
22. S. Ayik, B. Yilmaz, O. Yilmaz, and A. S. Umar, Quantal diffusion description of multinucleon transfers in heavy-ion collisions, *Phys. Rev. C* 97, 054618 (2018)
23. S. Ayik, B. Yilmaz, O. Yilmaz, A. S. Umar, and G. Turan, Multinucleon transfer in central collisions of ^{238}U +^{238} U, *Phys. Rev. C* 96, 024611 (2017)
24. R. Bass, Nuclear Reactions with Heavy Ions, Berlin, Heidelberg: Springer, 2010
25. C. J. Lin, Heavy-Ion Nuclear Reactions, Harbin Engineering Unirersity Press, Harbin, 2015
26. V. W. Oertzen, H. G. Bohlen, B. Gebauer, R. Künkel, F. Pühlhofer, and D. Scühll, Quasi-elastic neutron transfer and pairing effects in the interaction of heavy nuclei, *Z. Phys. A* 326, 463 (1987)
27. V. W. Oertzen, Cold multi-nucleon transfer between heavy nuclei and the synthesis of new elements, *Z. Phys. A* 342, 177 (1992)
28. F. L. H. Wolfs, Fission and deep-inelastic scattering yields for ^{58}Ni+^{112,124}Sn sn at energies around the barrier, *Phys. Rev. C* 36, 1379 (1987)
29. L. Corradi, A. M. Stefanini, C. J. Lin, S. Beghini, G. Montagnoli, F. Scarlassara, G. Pollarolo, and A. Winther, Multinucleon transfer processes in ^{64}Ni+^{238}U, *Phys. Rev. C* 59, 261 (1999)
30. L. Corradi, G. Pollarolo, and S. Szilner, Multinucleon transfer processes in heavy-ion reactions, *J. Phys. G* 36, 113101 (2009)

31. R. Kaufmann and R. Wolfgang, Complex nucleon transfer reactions of heavy ions, *Phys. Rev. Lett.* 3, 232 (1959)

32. R. W. Hasse, Approaches to nuclear friction, *Rep. Prog. Phys.* 41, 1027 (1978)

33. D. H. E. Gross and H. Kalinowski, Friction model of heavy-ion collisions, *Phys. Rep.* 45, 175 (1978)

34. W. Nörenberg, Transport phenomena in multi-nucleon transfer reactions, *Phys. Lett. B* 52, 289 (1974)

35. J. Galin, D. Guerreau, M. Lefort, J. Peter, X. Tarrago, and R. Basile, Mechanism of single-nucleon and multi-nucleon transfer reactions in grazing collisions of heavy ions on silver, *Nucl. Phys. A* 159, 461 (1970)

36. A. G. Artukh, G. F. Gridnev, V. L. Mikheev, and V. V. Volkov, New isotopes ^{22}O, ^{20}N and ^{18}C produced in transfer reactions with heavy ions, *Nucl. Phys. A* 137, 348 (1969)

37. A. G. Artukh, G. F. Gridnev, V. L. Mikheev, V. V. Volkov, and J. Wilczynski, Transfer reactions in the interaction of ^{40}Ar with ^{232}Th, *Nucl. Phys. A* 215, 91 (1973)

38. J. Wilczynski, Nuclear molecules and nuclear friction, *Phys. Lett. B* 47, 484 (1973)

39. B. Tamain, C. Ng, J. Pter, and F. Hanappe, Fission of medium and heavy nuclei induced by ^{40}Ar from 160 to 300 MeV: Cross sections, *Nucl. Phys. A* 252, 187 (1975)

40. P. Auger, T. H. Chiang, J. Galin, B. Gatty, D. Guerreau, E. Nolte, J. Pouthas, X. Tarrago, and J. Girard, Observation of new nuclides ^{37}Si, ^{40}P and ^{41}S, ^{42}S produced in deeply inelastic reactions induced by ^{40}Ar on ^{238}U, *Z. Phys. A* 289, 255 (1979)

41. D. Guerrau, J. Galin, B. Gatty, X. Tarrago, J. Girard, R. Lucas, and C. Ngô, Seven new neutron rich nuclides observed in deep inelastic collisions of 340 MeV ^{40}Ar on ^{238}U, *Z. Phys. A* 295, 105 (1980)

42. H. Breuer, K. L. Wolf, B. G. Glagola, K. K. Kwiatkowski, A. C. Mignerey, V. E. Viola, W. W. Wilcke, W. U. Schrder, J. R. Huizenga, D. Hilscher, and J. Birkelund, Production of neutron-excess nuclei in ^{56}Fe-induced reactions, *Phys. Rev. C* 22, 2454 (1980)

43. P. A. Söderström, J. Nyberg, P. H. Regan, A. Algora, G. de Angelis, et al., Spectroscopy of neutron-rich ^{168,170}Dy: Yrast band evolution close to the N_pN_n valence maximum, *Phys. Rev. C* 81, 034310 (2010)

44. H. Sophie, Multinucleon transfer reactions a pathway to new heavy and superheavy nuclei? *Phys. Conf. Ser.* 1014, 012005 (2018)

45. S. K. Allison, P. G. Murphy, and E. Norbeck, Mass of ^{13}B from the nuclear reaction ^{7}Li(^{7}Li, p)^{13}B, *Phy. Rev.* 102, 1182 (1956)

46. T. S. Bhatia, H. Hafner, R. Haupt, R. Maschuw, and G. J. Wagner, Masses of ^{62}Fe and the new isotope ^{68}Ni from (^{18}O+^{20}Ni) reactions, *Z. Phys. A* 281, 65 (1977)

47. P. Dessagne, M. Bernas, M. Langevin, G. C. Morrison, J. Payet, F. Pougheon, and P. Roussel, The complex transfer reaction (^{14}C, ^{15}O) on Ni, Zn and Ge targets: Existence and mass of ^{69}Ni, *Nucl. Phys. A* 426, 399 (1984)

48. K. Zhao, J. S. Lilley, P. V. Drumm, D. D. Warner, R. A. Cunningham, and J. N. Mo, Production of ^{199}Ir via exotic nucleon transfer reaction, *Chin. Phys. Lett.* 265 (1993)

49. L. Zhang, G. M. Jin, J. H. Zhao, W. F. Yang, Y. F. Yang, Z. Z. Zhao, J. W. Zheng, X. R. Sun, J. C. Wang, Z. W. Li, Z. Qin, G. H. Guo, Y. Luo, Z. Jan, and Z. Jingye, Observation of the new neutron-rich nuclide ^{208}Hg, *Phys. Rev. C* 49, R592 (1994)

50. S. Yuan, W. Yang, W. Mou, X. Zhang, Z. Li, X. Yu, J. Gu, Y. Guo, Z. Gan, H. Liu, and J. Guo, A new isotope of protactinium: ^{239}Pa, *Z. Phys. A* 352, 235 (1995)

51. L. Zhang, J. Zhao, J. Zheng, J. Wang, Z. Qin, Y. Yang, C. Zhang, G. Jin, G. Guo, Y. Du, T. Guo, T. Wang, B. Guo, J. Tian, and Y. Lou, Neutron-rich heavy residues and exotic multinucleon transfer, *Phys. Rev. C* 58, 156 (1998)

52. S. Yuan, W. Yang, Z. Li, J. He, T. Ma, K. Fang, S. Shen, Z. Gan, Q. Pan, Z. Chen, T. Guo, W. Mou, D. Su, Y. Xu, J. Guo, H. Liu, L. Shi, Z. Zhao, and H. Ma, Production and identification of a new heavy neutron-rich isotope ^{186}Hf, *Phys. Rev. C* 57, 1506 (1998)

53. J. He, W. Yang, S. Yuan, Y. Xu, Z. Li, T. Ma, B. Xiong, Z. Qin, W. Mou, Z. Gan, L. Shi, T. Guo, Z. Chen, and J. Guo, Synthesis and identification of a new heavy neutron-rich isotope ^{238}Th, *Phys. Rev. C* 59, 520 (1999)

54. C. Bruske, K. H. Burkard, W. Hller, R. Kirchner, O. Klepper, and E. Roeckl, Status report on the gsi on-line mass separator facility, *Nucl. Instr. Meth. Phys. Res. B* 186, 61 (1981)

55. K. L. Gippert, E. Runte, W. D. Schmidt-Ott, P. Tidemand-Petersson, N. Kaffrell, et al., Decay studies of neutron-rich radium and actinium isotopes, including the new nuclides ^{232}Ra and ^{232,234}Ac, *Nucl. Phys. A* 453, 1 (1986)

56. R. M. Chasteler, J. M. Nitschke, R. B. Firestone, K. S. Vierinen, P. A. Wilmarth, and A. A. Shihab-Eldin, Identification of the neutron-rich isotope ^{174}Er, *Z. Phys. A* 332, 239 (1989)

57. R. M. Chasteler, J. M. Nitschke, R. B. Firestone, K. S. Vierinen, and P. A. Wilmarth, Decay of the neutron-rich isotope ^{171}Ho and the identification of ^{169}Dy, *Phys. Rev. C* 42, R1171 (1990)

58. L. Corradi, J. H. He, D. Ackermann, A. M. Stefanini, A. Pisent, et al., Multinucleon transfer reactions in ^{40}Ca+^{124}Sn, *Phys. Rev. C* 54, 201 (1996)

59. L. Corradi, Evidence of complex degrees of freedom in multinucleon transfer reactions of ^{48}Ca+^{124}Sn, *Phys. Rev. C* 56, 938 (1997)

60. A. M. Stefanini, L. Corradi, G. Maron, A. Pisent, M. Trotta, et al., The heavy-ion magnetic spectrometer prisma, *Nucl. Phys. A* 701, 217 (2002)
61. H. Savajols, Vamos: A variable mode high acceptance spectrometer, *Nucl. Phys. A* 654, 1027c (1999)
62. A. Cunsolo, F. Cappuzzello, A. Foti, A. Lazzaro, A. L. Melita, et al., Technique for 1st order design of a large-acceptance magnetic spectrometer, *Nucl. Instrum. Methods Phys. Res* 481, 48 (2002)
63. L. Corradi, Heavy ion transfer reactions: Ongoing and future experiments performed with large acceptance magnetic spectrometers, *EPJ Web Conf.* 63, 02002 (2013)
64. L. Corradi, A. M. Vinodkumar, A. M. Stefanini, E. Fioretto, G. Prete, et al., Light and heavy transfer products in ^{58}Ni+^{208}Pb at the coulomb barrier, *Phys. Rev. C* 66, 024606 (2002)
65. S. Szilner, L. Corradi, G. Pollarolo, S. Beghini, B. R. Behera, et al., Multinucleon transfer processes in ^{40}Ca +^{208} Pb, *Phys. Rev. C* 71, 044610 (2005)
66. D. Montanari, L. Corradi, S. Szilner, G. Pollarolo, E. Fioretto, et al., Neutron pair transfer in ^{60}Ni+^{116}Sn far below the coulomb barrier, *Phys. Rev. Lett.* 113, 052501 (2014)
67. M. Evers, M. Dasgupta, D. J. Hinde, and C. Simenel, Multi-nucleon transfer in the reactions ^{16}O, ^{32}S+^{208}Pb, *EPJ Web Conf.* 17 (2011)
68. R. Broda, C. T. Zhang, P. Kleinheinz, R. Menegazzo, K. H. Maier, H. Grawe, M. Schramm, R. Schubart, M. Lach, and S. Hofmann, Collisions between ^{106}Cd and ^{54}Fe at 30 MeV above the coulomb barrier by high resolution $\gamma\gamma$ coincidences, *Phys. Rev. C* 49, R575 (1994)
69. R. Broda, Spectroscopic studies with the use of deep-inelastic heavy-ion reactions, *J. Phys. G* 32, R151 (2006)
70. C. H. Dasso, G. Pollarolo, and A. Winther, Systematics of isotope production with radioactive beams, *Phys. Rev. Lett.* 73, 1907 (1994)
71. G. G. Adamian, N. V. Antonenko, and A. S. Zubov, Production of unknown transactinides in asymmetry-exit-channel quasifission reactions, *Phys. Rev. C* 71, 034603 (2005)
72. V. Zagrebaev and W. Greiner, Production of new heavy isotopes in low-energy multinucleon transfer reactions, *Phys. Rev. Lett.* 101, 122701 (2008)
73. Z. Q. Feng, G. M. Jin, and J. Q. Li, Production of heavy isotopes in transfer reactions by collisions of ^{238}U+^{238}U, *Phys. Rev. C* 80, 067601 (2009)
74. G. G. Adamian, N. V. Antonenko, V. V. Sargsyan, and W. Scheid, Possibility of production of neutron-rich zn and ge isotopes in multinucleon transfer reactions at low energies, *Phys. Rev. C* 81, 024604 (2010)
75. G. G. Adamian, N. V. Antonenko, V. V. Sargsyan, and W. Scheid, Predicted yields of new neutron-rich isotopes of nuclei with $z = 64 - 80$ in the multinucleon transfer reaction ^{48}Ca +^{238} U, *Phys. Rev. C* 81, 057602 (2010)
76. Y. X. Watanabe, Y. H. Kim, S. C. Jeong, Y. Hirayama, N. Imai, et al., Pathway for the production of neutron-rich isotopes around the $N = 126$ shell closure, *Phys. Rev. Lett.* 115, 172503 (2015)
77. V. F. Comas, S. Heinz, S. Hofmann, D. Ackermann, J. A. Heredia, F. P. Heßberger, J. Khuyagbaatar, B. Kindler, B. Lommel, and R. Mann, Study of multinucleon transfer reactions in ^{58,64}Ni+^{207}Pb collisions at the velocity filter ship, *Eur. Phys. J. A* 49, 1 (2013)
78. E. M. Kozulin, E. Vardaci, G. N. Knyazheva, A. A. Bogachev, S. N. Dmitriev, et al., Mass distributions of the system ^{136}Xe + ^{208}Pb at laboratory energies around the coulomb barrier: A candidate reaction for the production of neutron-rich nuclei at N = 126, *Phys. Rev. C* 86, 044611 (2012)
79. J. V. Kratz, M. Schädel, and H. W. Gäggeler, Reexamining the heavy-ion reactions ^{238}U+^{238}U and ^{238}U+^{248}Cm and actinide production close to the barrier, *Phys. Rev. C* 88, 054615 (2013)
80. J. S. Barrett, W. Loveland, R. Yanez, S. Zhu, A. D. Ayangeakaa, et al., ^{136}Xe +^{208} Pb reaction: A test of models of multinucleon transfer reactions, *Phys. Rev. C* 91, 064615 (2015)
81. A. Vogt, M. Siciliano, B. Birkenbach, P. Reiter, K. Hadyska-Klk, et al., High-spin structures in ^{132}Xe and ^{133}Xe and evidence for isomers along the $N = 79$ isotones, *Phys. Rev. C* 96, 024321 (2017)
82. E. M. Kozulin, V. I. Zagrebaev, G. N. Knyazheva, I. M. Itkis, K. V. Novikov, M. G. Itkis, S. N. Dmitriev, I. M. Harca, A. E. Bondarchenko, A. V. Karpov, V. V. Saiko, and E. Vardaci, Inverse quasifission in the reactions ^{156,160}Gd+^{186}W, *Phys. Rev. C* 96, 064621 (2017)
83. V. I. Zagrebaev, Y. T. Oganessian, M. G. Itkis, and W. Greiner, Superheavy nuclei and quasi-atoms produced in collisions of transuranium ions, *Phys. Rev. C* 73, 031602 (2006)
84. J. V. Kratz, W. Loveland, and K. J. Moody, Syntheses of transuranium isotopes with atomic numbers $Z \leq 103$ in multi-nucleon transfer reactions, *Nucl. Phys. A* 944, 117 (2015)
85. M. Schädel, Prospects of heavy and superheavy element production via inelastic nucleus-nucleus collisions from ^{238}U+^{238}U to ^{18}O+^{254}Es, *EPJ Web Conf.* 131, 04001 (2016)
86. A. Vogt, B. Birkenbach, P. Reiter, L. Corradi, T. Mijatović, et al., Light and heavy transfer products in ^{136}Xe+^{238}U multinucleon transfer reactions, *Phys. Rev. C* 92, 024619 (2015)
87. H. M. Devaraja, S. Heinz, O. Beliuskina, V. Comas, S. Hofmann, et al., Observation of new neutron-deficient isotopes with $Z \geq 92$ in multinucleon transfer reactions, *Phys. Lett. B* 748, 199 (2015)
88. H. Gäggeler, W. Brüchle, M. Brügger, M. Schädel, K. Smmerer, et al., Production of cold target-like fragments in the reaction of ^{48}Ca+^{248}Cm, *Phys. Rev. C* 33, 1983 (1986)

89. N. V. Antonenko, E. A. Cherepanov, A. K. Nasirov, V. P. Permjakov, V. V. Volkov, Competition between complete fusion and quasi-fission in reactions between massive nuclei: The fusion barrier, *Phys. Lett. B* 319, 425 (1993)
90. G. G. Adamian, N. V. Antonenko, W. Scheid, Model of competition between fusion and quasifission in reactions with heavy nuclei, *Nucl. Phys. A* 618, 176 (1997)
91. Yu. E. Penionzhkevich, G. G. Adamian, N. V. Antonenko, Towards neutron drip line via transfer-type reactions, *Phys. Lett. B* 621, 119 (2005)
92. L. Zhu, J. Su, and P. W. Wen, Optimal incident energies for production of neutron-deficient actinide nuclei in the reaction ^{58}Ni $+^{238}$ U, *Phys. Rev. C* 95, 044608 (2017)
93. L. Zhu, Z. Q. Feng, and F. S. Zhang, Production of heavy neutron-rich nuclei in transfer reactions within the dinuclear system mode, *J. Phys. G* 42, 085102 (2015)
94. R. J. Charity, Systematic description of evaporation spectra for light and heavy compound nuclei, *Phys. Rev. C* 82, 014610 (2010)
95. L. Zhu, J. Su, W. J. Xie, and F. S. Zhang, Theoretical study on production of heavy neutron-rich isotopes around the $N = 126$ shell closure in radioactive beam induced transfer reactions, *Phys. Lett. B* 767, 437 (2017)
96. M. Schädel, et al., Actinide production in collisions of ^{238}U with ^{248}Cm, *Phys. Rev. Lett.* 48, 852 (1982)
97. L. Zhu, J. Su, W. J. Xie, and F. S. Zhang, Production of neutron-rich transcalifornium nuclei in ^{238}U-induced transfer reactions, *Phys. Rev. C* 94, 054606 (2016)
98. L. Zhu, Theoretical study on production cross sections of exotic actinide nuclei in multinucleon transfer reactions, *Chin. Phys. C* 41, 124102 (2017)
99. A. Winther, Grazing reactions in collisions between heavy nuclei, *Nucl. Phys. A* 572, 191 (1994)
100. A. Winther, Dissipation, polarization and fluctuation in grazing heavy-ion collisions and the boundary to the chaotic regime, *Nucl. Phys. A* 594, 203 (1995)
101. http://nrv.jinr.ru/nrv/webnrv/grazing/
102. http://personalpages.to.infn.it/∼nanni/grazing/
103. P. W. Wen, C. Li, L. Zhu, C. J. Lin, and F. S. Zhang, Mechanism of multinucleon transfer reaction based on the GRAZING model and DNS model, *J. Phys. G* 44, 115101 (2017)
104. J. Aichelin, "Quantum" molecular dynamics-a dynamical microscopic n-body approach to investigate fragment formation and the nuclear equation of state in heavy ion collisions, *Phys. Rep.* 202, 233 (1991)
105. N. Wang, Z. X. Li, and X. Z. Wu, Improved quantum molecular dynamics model and its applications to fusion reaction near barrier, *Phys. Rev. C* 65, 064608 (2002)
106. C. Li, J. L. Tian, L. Ou, and N. Wang, Finite-size effects on fragmentation in heavy-ion collisions, *Phys. Rev. C* 87, 064615 (2013)
107. C. Li, F. Zhang, J. J. Li, L. Zhu, J. L. Tian, N. Wang, and F. S. Zhang, Multinucleon transfer in the ^{136}Xe+ ^{208}Pb reaction, *Phys. Rev. C* 93, 014618 (2016)
108. C. Li, P. W. Wen, J. J. Li, G. Zhang, B. Li, X. X. Xu, Z. Liu, S. F. Zhu, and F. S. Zhang, Production mechanism of new neutron-rich heavy nuclei in the ^{136}Xe $+^{198}$ Pt reaction, *Phys. Lett. B* 776, 278 (2018)
109. L. Zhu, F. S. Zhang, P. W. Wen, J. Su, and W. J. Xie, Production of neutron-rich nuclei with $Z = 60-73$ in reactions induced by Xe isotopes, *Phys. Rev. C* 96, 024606 (2017)
110. G. Zhang, C. Li, P. W. Wen, J. J. Li, X. X. Xu, B. Li, Z. Liu, and F. S. Zhang, Production of neutron-rich $^{209-212}$Pt isotopes based on a dinuclear system model, *Phys. Rev. C* 98, 014603 (2018)